Physica D 57 (1992) 267–282
North-Holland

PHYSICA D

Localized breather-like solution in a discrete Klein–Gordon model and application to DNA

T. Dauxois, M. Peyrard
Laboratoire OSC, Université de Bourgogne, 6 Bd Gabriel, 21000 Dijon, France

and

C.R. Willis
Department of Physics, Boston University, 590 Commonwealth Ave, Boston, MA 02215, USA

Received 4 February 1992
Accepted 10 April 1992
Communicated by H. Flaschka

Non-propagating localized oscillating solutions are studied in the case of a discrete one-dimensional system with the 2–3 power onsite potential. A multiple-scale asymptotic perturbation expansion is not adequate for describing the large amplitude oscillations we consider. Starting from an exact pulse-like solution in the continuum, we derive an approximate oscillating solution. Our numerical simulations reveal that, whereas the excitations are strongly damped in the strong intersite coupling case, they are long-lived in the discrete cases. An additional modulation phenomenon of the oscillation, seen in the simulation, is explained by combination of the breather oscillations with the zero group velocity phonons modes. Then, applying the Green's functions formalism in analogy with a previous work (S. Takeno et al., Prog. Theor. Phys. Suppl. 94 (1988)), we derive a very accurate expression for the discrete breather with a quasi-infinite lifetime. Lastly, we demonstrate how such excitations can explain why the breathers make the dominant contributions in the dynamics of a simple model of DNA.

1. Introduction

Over the past several years, it has become increasingly apparent that spatially localized, oscillating nonlinear excitations contribute significantly to the behavior of biological structures. In order to model the fluctuational opening of DNA, we are interested in localized oscillating nonlinear wave-like solutions which are periodic in time, i.e. in the continuum limit we consider an equation of the form

$$u_{tt} - u_{xx} + f(u) = 0\,, \tag{1.1}$$

and we look for solutions verifying $u(x, T + t) = u(x, t)$, $\lim_{|x|\to\infty} u = 0$ and $u_t \not\equiv 0$. The sine-Gordon equation is singled out among nonlinear wave equation of type (1.1) because it has such a solution: the breather can be thought of as a "bound state" of a kink and an antikink. On the other hand, the ϕ^4 model does not possess breather solutions. In a letter [1], a proof of nonexistence of small-amplitude breather solutions to the well-known ϕ^4 equation was given by Segur and Kruskal. Starting with a formal expansion for the breather solution [2] and using the method of matched asymptotic expansions, they find a correction to the solution lying beyond all orders of the expansion which is not localized in space. So, even though the expansion itself is valid to all orders, ϕ^4 theory admits no true breathers. Maslov has found that, in the

continuum approximation, the Klein–Gordon equation with a logarithmic nonlinearity is the only one which permits exact solutions of pulson type [3].

However, one must also consider the discreteness of the lattice: it is an intrinsic feature of many physical systems which is generally ignored for the sake of simplicity. However, it seems that the opening of base-pairs of double stranded DNA are extremely localized [4,5] (typically just a few base-pairs are concerned), so that discreteness effects should be very important and could be the fundamental reason of the stability of a localized solution as evoked in some papers [6–8] and confirmed by our following results. The discreteness effects have been essentially investigated in the prototype Frenkel–Kontorova model, and generally in systems bearing topological nonlinear excitations. Recently, using a collective-variable theory [9], Boesch and Peyrard described the dynamics of discrete SG breather. They derived expressions for the total energy of the system and the effective potential for the collective variable, both of which explicitly describe the competition between Peierls' wells and the subkink interaction energy. Elsewhere, Campbell and Peyrard [10] showed that, in the ϕ^4 theory, the conclusions about breather instability derived from a continuous model cannot be trivially extended to a discrete system. They present new numerical results which show an "intricate interweaving" of stable and unstable breather solutions on finite discrete lattices.

We therefore ask a basic question: how is it possible to exhibit a localized breather-like excitation in a discrete lattice? We are guided by the continuum SG breather which is a sum of a kink and an antikink. A possibly simple way to generate oscillating solutions is to investigate a "head-on" collision between a kink and an antikink solution [11,12] in a nonintegrable system. This is fairly easy to carry out in the ϕ^4 model for example, but we consider below a model with a substrate potential with only one stable equilibrium position, and therefore without topological solitons: the breathers cannot be thought of as a bound state of topological solitons. Consequently, we have to find another scheme to exhibit breather-like excitations. First, by analogy with the SG theory where the small amplitude form of the SG breather can be understood in terms of a "multiple-scale" perturbation expansion, we consider a NLS soliton. However, the resulting solution for our case is not valid for a large enough amplitude to provide a description of DNA breathing modes. We therefore start from a static pulse-like solution obtained in the continuum limit, multiplied by a periodic function. This method yields an approximate solution for a breatherlike object. However numerical simulations show that in the strong intersite coupling regime, the coupling between the oscillatory and phonon modes induces a strong damping of the oscillations. But in the discrete case the solution turns out to be much more stable, suggesting that, if the initial conditions were carefully chosen, stable breathers could be formed.

The idea that discreteness effects could stabilize a breather has recently been developed in the context of self-localized vibrational modes induced by anharmonicity in pure crystals. Takeno and coworkers [13] employed the lattice Green's functions method to show the existence of on an s-like symmetry mode induced by quartic anharmonicity in discrete systems, in close analogy with the case of a localized mode due to an impurity atom or force constant defect in the harmonic lattices. The localized mode obtained is a new kind of stable bound state, which *does not* exist in the continuum case. It is a particle-like mode unattainable from the perturbation theory or the self-consistent theory, because the frequency of this new type of soliton-like mode lies outside the phonon band, so that the breather-like oscillations cannot be coupled with the phonons. Following the same idea, we assume that the discreteness could be a necessary condition for our system to bear such a localized mode and we apply the theory of Takeno et al. to harmonic lattices with a nonlinear on-site

potential. Seeking stationary solutions with an appropriate shape, suggested by the numerical simulations, and using the lattice Green's functions formalism, we exhibit solutions that are in an excellent agreement with numerical results. The extremely weak radiation of these approximate breathers suggests that even though we have not imposed the condition of indestructibility, related to the mathematical problem of the complete integrability of the system, one would expect to see such long-lived breather-like objects in physical applications.

Guided by the idea that nonlinear effects might concentrate vibrational energy in DNA into a localized packet, as assumed by many models [6,14,15], we propose breathing modes as a model for the fluctuational openings suggested by experiments [16–18]. The parameters lead to a very discrete behavior, which gives rise to static solitary excitations which are physically relevant according to an estimate of the ratio of the energy of a breather in comparison with the thermal energy. We explain why the breathers make the dominant contributions in DNA, as indicated by some simulations.

The remainder of the paper is organized as follows. In section 2 we present the model, the phonon modes and the small amplitude approximate breather solution of the discrete equation of motion. In section 3, we then specialize our study to the continuum case, in order to derive expressions for a non-propagative breather. We devote section 4 entirely to the results of the numerical simulations and show first how the discreteness could be favorable to a quasi-infinite breather lifetime and second that we get a rather good static oscillating profile in the discrete cases. In section 5 we present an outline of the Green's functions formalism to determine more precisely the static breather and the results are then compared with the previous ones. In section 6 we discuss the possible implications of our analysis for the existence of breathing modes in a simple model of DNA. In the last section, we present our concluding remarks.

We limit ourselves to breather modes which do not move along the lattice to avoid additional discreteness effects due to their propagation. Except in section 3, we focus our attention on very localized breathers, spanning only a few units of the lattice, so that our calculations treat intrinsically the discreteness.

2. Model and excitations of the system

2.1. Presentation of the system

The discrete model that we consider consists of a chain of particles of mass m, with the lattice spacing l along the z axis and submitted to the substrate potential (cf. fig. 1)

$$V(y_n) = D(\tfrac{1}{2}y_n^2 - \alpha \cdot \tfrac{1}{3}y_n^3),$$

where D is the constant for the on-site potential energy, α fixes the relative width of the well and y_n the transversal displacement of the nth particle from its equilibrium position. The potential was chosen because it represents qualitatively a potential with a hard repulsive part and a softer attractive part as in most of the chemical bonds. It diverges as y_n goes to infinity, which would be a problem in statistical mechanics, but as we are interested in localized oscillating solutions, with an amplitude which is beyond the breaking of

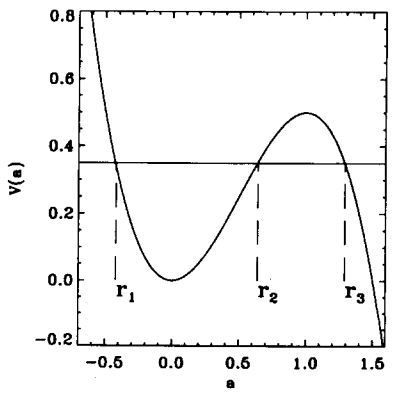

Fig. 1. Substrate potential $V(a)$, with the definitions of the three roots r_1, r_2, r_3 defined in section 3.

the chemical bonds, we will restrict ourselves to the region inside the well (i.e. $\alpha y_n \in [-0.5, 1]$), except in section 3, where we exhibit an exact but unstable soliton solution.

Nearest neighbouring particles are harmonically coupled with elastic coefficient k so that the Hamiltonian of the system is

$$H = \sum_n \left[\tfrac{1}{2} m \dot{y}_n^2 + \tfrac{1}{2} k (y_n - y_{n-1})^2 + V(y_n)\right], \quad (2.1)$$

where the first term is the kinetic energy (y_n dot denotes the time derivative). Let us define dimensionless variables describing the transverse displacements in terms of $u_n = \alpha y_n$, the distance along the chain by $\xi = z/l$ and the scaled time $\tau = t\sqrt{k/m}$; the dimensionless parameter

$$\omega_d^2 = \frac{D}{k}$$

determines the ratio of the on-site potential energy to the elastic coupling energy. With this more appropriate system of units, we get the following form for the Hamiltonian:

$$H = \frac{k}{\alpha^2} \sum_n \left[\tfrac{1}{2} \dot{u}_n^2 + \tfrac{1}{2} (u_n - u_{n-1})^2 + \omega_d^2 (\tfrac{1}{2} u_n^2 - \tfrac{1}{3} u_n^3)\right]. \quad (2.2)$$

The corresponding equation of motion in dimensionless form is

$$\ddot{u}_n - (u_{n+1} + u_{n-1} - 2u_n) + \omega_d^2 (u_n - u_n^2) = 0. \quad (2.3)$$

The displacive regime of (2.3) is obtained when the displacements field does not change drastically over a lattice spacing (i.e. there is a strong intersite interaction, $\omega_d \ll 1$) and extended lattices modes determine the physics. When $\omega_d > 1$, we are in the discrete regime where the continuum limit approximation is not valid.

2.2. *Oscillating solutions of the system*

We first discuss the solutions of the harmonic limit, which correspond to the small amplitude oscillations or "phonons" in the bottom of the potential well. Keeping only linear terms in eq. (2.3), we can easily obtain the linear solutions, assuming they have the form of plane waves $f(\tau) = A\, e^{i(qn - \omega\tau)}$ where A is a constant amplitude (required to be infinitesimally small), q the wave vector and ω the frequency. Substituting into the harmonic limit of (2.3), we obtain the dispersion law for linear vibrations

$$\omega^2(q) = \omega_d^2 + 4 \sin^2(\tfrac{1}{2} q). \quad (2.4)$$

It is a dispersion relation, corresponding to an optical branch, in the sense $\lim_{|q| \to 0} \omega \neq 0$. The linear group velocity is $V_g = \sin(q)/\omega(q)$. However, as explained, we are interested not only in really nonlinear solutions, but also in localized vibrations. Considering, as first step, only weakly nonlinear solutions, we can apply the classical multiple scale expansion [19] to provide an asymptotic perturbation expansion in the amplitude of the breather, working to lowest order in a small scaling parameter ε, and expanding the lowest order solution u_n, as the following spatially localized time-periodic form:

$$u_n(\tau) = \varepsilon [F_{1,n}(\varepsilon\tau)\, e^{i\theta_n} + \text{c.c.}] + \varepsilon^2 [F_{0,n}(\varepsilon\tau) + F_{2,n}(\varepsilon\tau)\, e^{i2\theta_n} + \text{c.c.}] + O(\varepsilon^3), \quad (2.5)$$

where we use $\theta_n = qn - \omega\tau$. Here the expansion is restricted to the order $O(\varepsilon^3)$, and c.c. means the complex conjugate. The functions $F_{i,n}$ are assumed to be slowly varying in time and from site to site: they can be determined in the continuum limit, while the fast oscillations of the quasiharmonic carrier, inside the envelope, are treated exactly. Following the standard reductive perturbation method and using the new variables $T = \varepsilon^2 \tau$ and $S = \xi - V_g \varepsilon \tau$, we obtain the well-known nonlinear Schrödinger (NLS) equation:

$$i F_{1,T} + P F_{1,SS} + Q |F_1|^2 F_1 = 0, \quad (2.6)$$

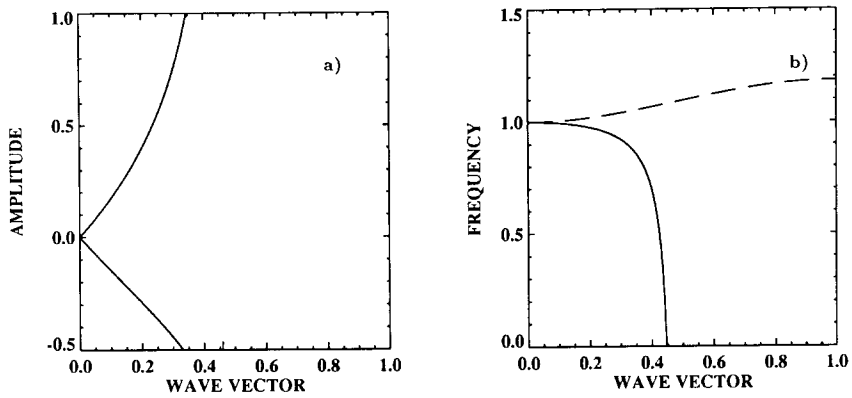

Fig. 2. (a) The maximum and the minimum of the amplitude for the small amplitude solutions versus the normalized wave vector. (b) The frequency ω_b (solid curve) and the dispersion relation $\omega(q)$ (dotted curve), in ω_d unit, versus the normalized wave vector. The discreteness parameter is $\omega_d^2 = 10$.

The nonlinearity and the dispersion parameter are given by

$$Q = \frac{\omega_d^2}{\omega} \frac{5\omega_d^2 + 32\sin^4(\frac{1}{2}q)}{3\omega_d^2 + 16\sin^4(\frac{1}{2}q)}$$

and

$$P = \frac{\omega_d^2 \cos(q) - 4\sin^4(\frac{1}{2}q)}{2\omega^3} .$$

For negative values of PQ, (2.6) has a solution, called dark-soliton, which has not the appropriate shape to represent breather modes. For positive values, the equation has an envelope-soliton solution. Here Q is always positive, whereas P is positive for $0 \le q \le q_0$, where q_0 correspond to the zero-dispersion point given by

$$\cos(q_0) = 1 - \frac{2}{1 + \sqrt{1 + 4/\omega_d^2}} .$$

The small amplitude breather expression, approximate solution of (2.3) is

$$u_n(\tau) = 2\varepsilon A \operatorname{sech}[\varepsilon(n - V_e\tau)/L_e] \times \Big[\cos(\Theta n - \omega_b \tau) + \varepsilon A \operatorname{sech}[\varepsilon(n - V_e\tau)/L_e] \times \Big(1 - \frac{1}{3 + 16/\omega_d^2 \sin^4(\frac{1}{2}q)} \times \cos[2(\Theta n - \omega_b\tau)]\Big)\Big] + O(\varepsilon^3) , \quad (2.7)$$

with

$$A = \sqrt{\frac{u_e^2 - 2u_e u_c}{2PQ}} , \quad L_e = \frac{2P}{\sqrt{u_e^2 - 2u_e u_c}} ,$$
$$V_e = V_g + \varepsilon u_e , \quad \Theta = q + \varepsilon u_e/2P ,$$
$$\omega_b = \omega + (V_g + u_c\varepsilon)\varepsilon u_e/2P ,$$

u_e and u_c the velocities of the envelope and carrier waves. As we will consider discrete breathers such that the center of mass of the breather is at rest in the laboratory frame[#1] (to prevent discreteness effects, such as Peierls–Nabarro additional potential), we should have $V_e = 0$. Taking $u_c = 0$, we obtain $\omega_b = \omega - V_g^2/2P < \omega$.

The solution (2.7) describes an oscillating localized wave packet, the oscillations of which are not symmetric due to the asymmetry of the on-site potential. Fig. 2 shows the amplitude and

[#1] It is possible to find a static solution of the NLS equation [20], but the final solution will be a propagating wave, because of the choice of the moving frame ($V_g \neq 0$).

frequencies of the breather solutions as a function of q. Large amplitude solutions can only be obtained when the breather frequency ω_b is well below the frequency ω of the phonons modes. But this is a domain where the multiple scale expansion breaks down. Therefore, although the method can provide analytical solutions taking discreteness into account, it is not appropriate for the type of solutions we are seeking.

3. Large amplitude solutions

The other conventional approach in the prospecting for breather modes in nonlinear equations consists in neglecting the discreteness to consider, in counterpart, large amplitude nonlinear excitations. We assume in this section that the coupling is strong enough to ensure that the variations of u from site to site are quite small. In this limit, we may replace u_n depending on the site index n by a continuous variable u, function of ξ and τ. This continuum approximation replaces the discrete set of equations (2.3) by the following partial differential equation:

$$u_{\tau\tau} - u_{\xi\xi} + \omega_d^2(u - u^2) = 0 . \qquad (3.1)$$

In this limit, the system is invariant under any translation along the ξ axis.

An exact pulse solution of the continuum 2–3 equation can be obtained directly by integration of the ordinary differential equation that results from assuming a traveling wave solution, with a speed β. It has the form

$$u = \tfrac{3}{2}\,\mathrm{sech}^2\left(\frac{\omega_d}{2\sqrt{1-\beta^2}}\,(\xi - \beta\tau)\right),$$

Since the solution approaches 0 as $|\xi| \to +\infty$, it describes a pulse in the u field, localized around $\xi = \beta\tau$. We denote by u_0 the static solution of the equation (3.1). The result is shown in fig. 3 where u is plotted against ξ for different values of ω_d.

Given this exact solitary wave solution, it is natural to ask how it evolves if the amplitude is lower than $\frac{3}{2}$. So we now look for solution of the form $u = a(\tau)u_0(\xi)$. Inserting this expression in (3.1), we get

$$\ddot{a}u_0 - a u_{0\xi\xi} + \omega_d^2(a u_0 - a^2 u_0^2) = 0 ,$$

i.e.

$$\ddot{a}u_0 + a(\tau)[-u_{0\xi\xi} + \omega_d^2(u_0 - u_0^2)] + \omega_d^2 u_0^2(a - a^2) = 0 .$$

As the bracket vanishes identically, we have by integration on the space variable from $-\infty$ to $+\infty$

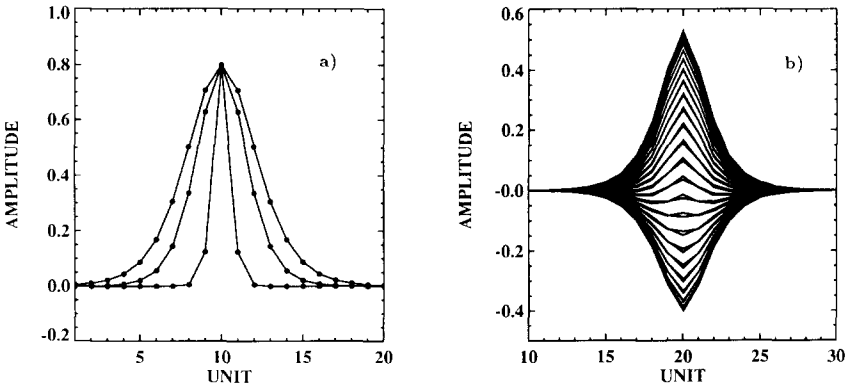

Fig. 3. Profile of the solutions. (a) Profile for the analytical solutions u_0 as function of unit of the lattice ($\omega_d^2 = 10, 1, 0.5$). (b) Breather oscillations in the case $\omega_d = 1$. Note the asymmetry of the oscillations.

$$\ddot{a} + \omega_d^2(a - a^2) = 0 . \tag{3.2}$$

Finally, upon multiplying both sides of equation (3.2) by $\dot{a}$ and performing the time integral we have

$$\tfrac{1}{2}\dot{a}^2 = \tfrac{1}{3}\omega_d^2(a^3 - \tfrac{3}{2}a^2 + C) = \tfrac{1}{3}\omega_d^2 R(a) , \tag{3.3}$$

where C is just a constant of integration. This equation is just a virial theorem for an analogue particle. With this mechanical analogy, we can consider that the particle sees a potential $U(a) = -\tfrac{1}{3}\omega_d^2 R(a)$ with a local maximum at $a = 1$ and a local minimum at $a = 0$. Further, we are interested in a localized breather mode, which must have a finite energy and a localized energy density. In view of the form of the potential, its field a must belong to $]-0.5, 1[$. We call $r_1 \leq r_2 \leq r_3$ the three real roots of the three order polynomial $R(a)$, when $0 < C < \tfrac{1}{2}$. Once the particle leaves from $a = r_1$, it rolls up to $a = r_2$, and begins a periodic motion, except when $a = r_1 = -0.5$, where the particle tends only asymptotically to $a = r_2 = r_3 = 1$. The mechanical analogy helps us to conclude also that the static solution, which corresponds to $a = 1$, is an unstable soliton solution. Apart from this general considerations, one can also explicitly solve (3.3) by quadrature; we have

$$\frac{da}{d\tau} = \pm\omega_d\sqrt{\tfrac{2}{3}R(a)} .$$

Supposing $a = r_1$ at $\tau = 0$, and using $a = r_1 + (r_2 - r_1)\, s^2$ for the sake of convenience in performing the integration, we get

$$\int_{r_1}^{a} \frac{ds}{\sqrt{R(s)}} = \pm\omega_d\sqrt{\tfrac{2}{3}}\tau$$

$$= \int_0^{s_a} \frac{2ds}{\sqrt{(r_3 - r_1)(1 - s^2)(1 - k^2 s^2)}}$$

$$= \frac{2}{\sqrt{r_3 - r_1}} \operatorname{sn}^{-1}(s_a, k) ,$$

where $k^2 = (r_2 - r_1)/(r_3 - r_1) \in [0, 1]$ and $s_a = \sqrt{(a - r_1)/(r_2 - r_1)}$. If sn is the elliptic sine-function [21], the approximate solution of (3.1) is finally

$$u(\xi, \tau) = \tfrac{3}{2}\operatorname{sech}^2(\tfrac{1}{2}\omega_d\xi)\Big[r_1 + (r_2 - r_1) \times \operatorname{sn}^2\Big(\omega_d\sqrt{\frac{r_3 - r_1}{6}}\,\tau, \sqrt{\frac{r_2 - r_1}{r_3 - r_1}}\Big)\Big] . \tag{3.4}$$

Before testing this solution numerically, we calculate two important physical quantities: the frequency and the energy of this solution. The function sn^2 is periodic in $2K$, where K is the complete elliptic integral of modulus k:

$$K = \int_0^{\pi/2} \frac{d\theta}{\sqrt{1 - k^2\sin^2\theta}} = K(k) .$$

So $\operatorname{sn}^2(\omega_d\sqrt{\tfrac{1}{6}(r_3 - r_1)}u)$ has a period of $2K/\omega_d\sqrt{\tfrac{1}{6}(r_3 - r_1)}$, and therefore a frequency

$$\omega_b = \frac{\pi\omega_d}{K}\sqrt{\frac{r_3 - r_1}{6}} . \tag{3.5}$$

Let us now calculate, the limiting values:

$$\begin{aligned} &r_3 = r_2 && \Rightarrow \omega_b = 0 , \\ &r_2 = r_1 = 0 \text{ and } r_3 = \tfrac{3}{2} && \Rightarrow \omega_b = 1 . \end{aligned}$$

As shown by the fig. 4a, the vibrational mode is characterized by a frequency, which decreases rapidly near the critical amplitude $a = 1$. We have something like a *soft-mode*, which cannot be coupled with phonons, because its frequency is always in the gap.

When one excitation of the preceding type is present on the chain, the continuum expression of the Hamiltonian (2.2) can be computed at $\tau = 0$. It reads

$$E = \int_{-\infty}^{+\infty} d\xi\, \frac{k}{\alpha^2}\,[\tfrac{1}{2}u_\tau^2 + \tfrac{1}{2}u_\xi^2 + \omega_d^2(\tfrac{1}{2}u^2 - \tfrac{1}{3}u^3)]$$

$$= \tfrac{12}{5}\sqrt{kD}\Big(\frac{r_2}{\alpha}\Big)^2(\tfrac{3}{2} - r_2) = \tfrac{12}{5}\sqrt{kD}\,\frac{C}{\alpha^2} .$$

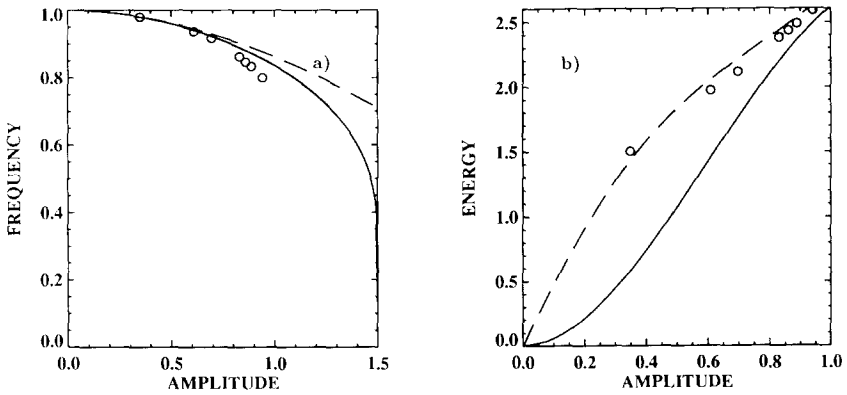

Fig. 4. Comparison of the NLS solution of section 2 (dotted curve) and the one obtained in the continuum limit of section 3 (solid curve). The dots are obtained using the Green's functions method. (a) The breather frequency versus the maximum amplitude of oscillation. The frequency is in ω_d unit, so the lower band edge of the phonons band corresponds to 1. (b) The breather energy versus the maximum amplitude of oscillation. The solid line energy is poor because the solution (3.4) is not the exact breather shape mode. The energy is in arbitrary units.

Fig. 4b shows the evolution of the energy versus the maximum of the amplitude of the solution and makes the comparison with the small amplitude one obtained in the preceding section.

4. Dynamics of a discrete breather

Our aim in this section is to study the properties of the solutions obtained analytically in section 3 and particularly their stability. We have developed a computer simulation program to study the behavior of the breather solutions in the system. In order to allow for an intrinsic treatment of the discreteness effects, numerical experiments are performed on the discrete system. Differential equations (2.3) with periodic conditions and specified initial conditions are solved using a fourth-order Runge–Kutta method.

In addition to the intrinsic spatial discretization such a numerical experimental involves a time discretization. The criterion for an appropriate choice of the time-step Δt and to test the accuracy of the integration method is that the total energy of the Hamiltonian system should remain constant during the computation. For Δt varying in the range 0.1–0.005, depending on the choice of ω_d, the change of the energy is less than 4×10^{-5} in relative value. The initial conditions for the displacements $u_n(0)$ and the velocities are deduced from the analytical solution (3.4). Since we are interested in nonlinear excitations the width of which is of the order of the lattice spacing, the preceding study in the continuum limit can only provide approximate solutions for a numerical study. We have considered here breather solutions such that the center of mass of the pulse is at rest in the laboratory frame, to avoid Peierls–Nabarro potential effects. We focus on the internal breathing motion, and not on the center of mass motion.

First of all, the solution with amplitude $\frac{3}{2}$ is clearly unstable in the numerical simulation, as expected. Therefore, limiting ourselves to solutions with an amplitude lower than 1, we obtain asymmetric oscillating solutions, whose localization is a function of the discreteness parameter ω_d. The asymmetry is due to the potential: the potential slope (force) is smaller in magnitude for positive values than for negative ones. Fig. 3b. Shows the profile of the solution at different times: its profile seems to *breathe*. The evolution of the solutions are shown in fig. 5. According to our results, we surprisingly found that the more

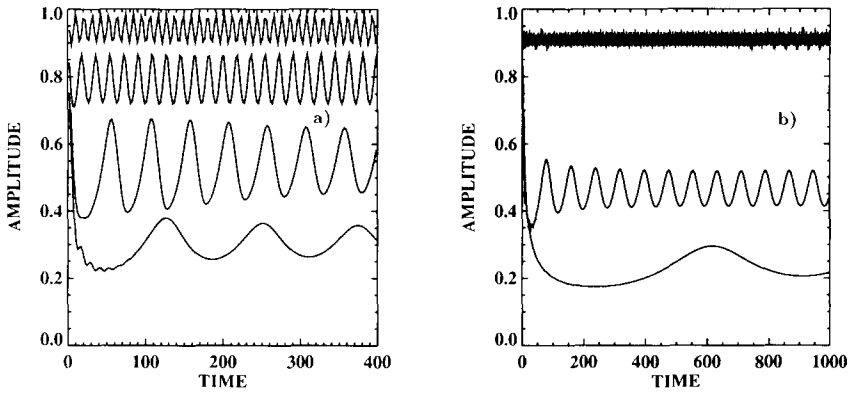

Fig. 5. The maxima of the wave amplitude as function of time. (a) For different initial amplitudes which are determined by the choice of C. In the decreasing order, the curves correspond to $C = 0.74, 0.65, 0.56, 0.5$. (b) For different values of ω_d but the same $C = 0.7$. In the decreasing order, the curves correspond to $\omega_d^2 = 15, 5, 1$.

discrete is the chain, the more stable is the solution obtained in the continuum limit (in fact, we can notice that each solution reaches a quasi-steady state, but in more discrete chains, the final amplitude is larger). One can ask whether discreteness effects could stabilize a time-dependent solution like the breather. In fact, the decay of the amplitude of the breather is caused by the radiation of energy out of the center. However, in a discrete model, the waves that can propagate have well defined frequencies lying in a finite width phonon band and thus a wave that should propagate in a continuum medium may decay exponentially in the corresponding discrete model. Furthermore, in agreement with what was found in section 3 and confirmed by our numerical results, the breather frequency lies always in the phonon gap, but because of the nonlinearity, all the multiples of the breather frequency will be present causing the breather motion to be damped. Nevertheless, for a more discrete system, the dispersion band is thinner so that the number of harmonics which can be coupled to phonons decreases, giving a larger breather lifetime.

Consider for example the solution in the case $\omega_d^2 = 10$ and $C = 0.7$. In a very short time (just a few oscillations), the amplitude goes from 0.955 to an average amplitude around 0.88. This drop is accompanied by the emission of a wave packet of rather large amplitude (called prompt radiation), simply because the initial state is not appropriate for the discrete chain. Therefore, it relaxes very fast to a modified shape, corresponding to a discrete breather. The resulting wave is sharply localized and only about 5 particles participate in the breathing motion. After this initial transient, small amplitude wave packets (called decay radiation) are symmetrically emitted from the pulse, which gives rise to a small damping of the breather, weak enough so that the breather can reach a quasi-steady state which corresponds to a rapid oscillation of frequency $\omega_b = \omega_d\ (0.836 \pm 0.006)$, slightly less than the initial condition, modulated by a smaller one of frequency $\omega_m = \omega_d\ (0.152 \pm 0.006)$. So the maximum amplitude pulsates with time at frequency ω_m, but around an apparent equilibrium amplitude.

The maxima of the amplitude at the center of the breather are shown in fig. 5a, as a function of time for different values of the initial amplitude. The difference between initial and final equilibrium amplitude decreases with the initial amplitude, whereas the frequency ω_m increases. A careful study of the frequency ω_b and the corresponding one ω_m, showed us that $\omega_b + \omega_m = \omega_d$ (0.99 ± 0.01). It suggested to us that the phenomenon of modulation is just a consequence of the inexact expression chosen as initial condi-

tion. The hypothesis is that the difference between the approximate solution and an exact hypothetical solution can be decomposed in terms of long wavelength phonon modes. Among these modes, the mode situated exactly at the bottom of the phonon band cannot be radiated away because its group velocity is zero[#2]. Therefore it stays and combines with the breather frequency through the nonlinear part of the equation to generate the frequencies $\omega_d + \omega_b$ and $\omega_d - \omega_b$, and generally all the combination modes, i.e. $(n\omega_d + m\omega_b)$ with $(n, m) \in \mathbb{Z}$. Because we plot the envelope of the breathing oscillation, the frequencies lower than ω_b are emphasized, whereas the largest ones seem to disappear: that is why we noticed the modulation phenomena, characterized by the frequency $\omega_d - \omega_b$. The temporal Fourier transform (c.f. fig. 6) of the motion of the center of the excitation confirms this hypothesis by the presence of the different frequency peaks. The same phenomenon was found, but not explained in an earlier paper [22]: the present explanation is valid for this case too.

It seems then clear that by extracting the undesirable frequency (analogue to the filtering in electronics) in the spectrum, and by leaving only the frequency ω_b and its harmonics, we can find the exact breather mode by performing the inverse Fourier transform of the resulting spectrum. We preferred however an analytical derivation of the solution.

5. Discrete breather solution

5.1. *The formalism of the Green's functions method*

The breathers modes considered above are very localized oscillating solutions whereas the displacements u_n were considered to be smooth functions in section 3, so that it was possible to use the continuum approximation directly. This is not the case for the excitations obtained when the discreteness parameter ω_d is large enough. This means that we must treat the u_n exactly. A technique for solving (2.3) is the Green's functions method. Much attention has been focused recently [13,23,24] on self-localized vibrational modes induced by the anharmonicity in pure crystal lattices. By introducing lattice Green's functions and using rotating wave approximation, analytical expressions were obtained. The profile of the anharmonic localized mode looks like an envelope soliton, but its nature is different from the conventional one, described for example by the NLS equation, because its existence becomes meaningless if we consider the continuum limit of the crystal lattice, and the theory is capable of elucidating the existence of a new type of modes with eigenfrequencies outside the harmonic frequency band.

In the previous section, we showed that the harmonic crystal lattice with nonlinear on-site potential can exhibit a self-localized mode below the harmonic frequency band unattainable from the multiple scales expansion. It is the purpose of this section to apply the lattice-Green functions theory of an s-like stationary self-localized mode in a one-dimensional (1D) lattice with nonlinear on-site potential. We seek long-lived oscillatory solutions to eq. (2.3). Stationary-mode solutions can be sought by putting

$$u_n = \sum_{i=0}^{\infty} \phi_n^i \cos(i\omega_b t) , \tag{5.1}$$

where ω_b is the eigenfrequency of the fundamental model ($i = 1$) and ϕ_n^i are time independent amplitude of the ith mode (the ansatz has a dc part simply because of the asymmetry of the potential). We insert this ansatz in eq. (2.3), and set the coefficients of $\cos(i\omega_b t)$ equal to each other, retaining only the first three terms (we will show below that this is a good approximation).

[#2] Since the excitation of all the particles by the breather occurs essentially simultaneously (in phase) the excitation of the other static phonon frequencies ($\omega = \omega(\pm\pi)$) is extremely weak, and indistinguishable on the Fourier spectrum.

We obtain

$$\omega_d^2\phi_n^0 - (\phi_{n+1}^0 + \phi_{n-1}^0 - 2\phi_n^0) = \omega_d^2[\phi_n^{0^2} + \tfrac{1}{2}(\phi_n^{1^2} + \phi_n^{2^2})], \tag{5.2}$$

$$(\omega_d^2 - \omega_b^2)\phi_n^1 - (\phi_{n+1}^1 + \phi_{n-1}^1 - 2\phi_n^1) = \omega_d^2(2\phi_n^0 + \phi_n^2)\phi_n^1, \tag{5.3}$$

$$(\omega_d^2 - 4\omega_b^2)\phi_n^2 - (\phi_{n+1}^2 + \phi_{n-1}^2 - 2\phi_n^2) = \omega_d^2(2\phi_n^0\phi_n^2 + \tfrac{1}{2}\phi_n^{1^2}). \tag{5.4}$$

Here the Green's function is invoked to rewrite the equations in terms of 1D lattice Green's function, which may be written in terms of the normalized solutions of the linear part of the above equations,

$$G(n-m, \omega_b) = \omega_d^2 \frac{1}{N} \sum_q \frac{e^{iq(n-m)}}{\omega^2(q) - \omega_b^2} \tag{5.5}$$

where q is the wave vector inside the first Brillouin zone, and N the number of atoms. With $q = 0,\ \pm 2\pi/N,\ \pm 2\cdot 2\pi/N, \ldots, \pi$ (respectively $q = 0,\ \pm 2\pi/N,\ \pm 2\cdot 2\pi/N, \ldots, \pm(N-1)2\pi/N$) if N is even integer (respectively odd), it is easy to check that $\forall N$, $\Sigma_q \Sigma_n e^{i(q-q')n} = N$. Then, we get

$$\phi_n^0 = \sum_m G(n-m, 0)[\phi_m^{0^2} + \tfrac{1}{2}(\phi_m^{1^2} + \phi_m^{2^2})], \tag{5.6}$$

$$\phi_n^1 = \sum_m G(n-m, \omega_b)(2\phi_m^0 + \phi_m^2)\phi_m^1, \tag{5.7}$$

$$\phi_n^2 = \sum_m G(n-m, 2\omega_b)(2\phi_m^0\phi_m^2 + \tfrac{1}{2}\phi_m^{1^2}). \tag{5.8}$$

These equations constitute a set of simultaneous nonlinear eigenvalue equations determining the eigenfrequency ω_b and the eigenfunctions ϕ_n^i. Introducing the new variable $y = 1 + \frac{1}{2}(\omega_d^2 - \omega_b^2)$, we have

$$G(n, \omega_b) = \omega_d^2 \frac{1}{N} \sum_q \frac{e^{iqn}}{\omega_d^2 - \omega_b^2 + 2[1 - \cos(q)]} = \frac{\omega_d^2}{2N} \sum_q \frac{\cos(qn)}{y - \cos(q)}.$$

We are concerned here with a localized mode lying below the bottom of the harmonic frequency band ($\omega_b < \omega_d$). The nature of this particle like mode is entirely different from that of the conventional wave-like phonons modes. For y lying outside $[-1, 1]$ (i.e. ω_b below the phonon-band) the lattice Green's function $G(n, \omega_b)$ is non-singular. The calculation of $G(n, 2\omega_b)$ is different because in that case $y < 1$. But for $(2\omega_b)^2 > \omega^2(\pi) = \omega_d^2 + 4$, we have $y < -1$; so $1/[y - \cos(q)]$ has no pole. Physically the condition means that the harmonics of the fundamental oscillations ω_b should be out of the phonons band.

It is possible to obtain a simpler form in the case of large N, replacing the sum by an integral (see appendix A). The values obtained with the

Table 1
Results for the $\omega_d^2 = 10$ and $\omega_b = 0.837\ \omega_d$. Values of y, the Green's functions and the time-independent amplitude of the first three modes (S, F and G are respectively referring to the results of the Fourier transform (cf. fig. 6), the Fourier series of the solution (5.1) and the Green's functions formalism. Note that the first method does not give us the sign of the coefficients, although we can obtain it by Bayard and Bode's theorem.

	i		
	0	1	2
$y(i\omega_b)$	6	2.50	−8.00
$G(0, i\omega_b)$	0.8452	2.1834	−0.6296
$G(1, i\omega_b)$	0.0709	0.4559	0.0395
$G(2, i\omega_b)$	0.0060	0.0952	−0.0025
$G(3, i\omega_b)$	0.0005	0.0199	0.0002
ϕ_0^i S	0.28	±0.5	±0.11
ϕ_0^i F	0.2794	0.8185	−0.1131
ϕ_0^i G	0.2794	0.7196	−0.1191
ϕ_1^i S	0.039	±0.114	±0.0002
ϕ_1^i F	0.0435	0.1276	−0.0176
ϕ_1^i G	0.0435	0.1786	−0.0024

exact discrete expression for $G(n, \omega_b)$ (when $N = 100$) and the one obtained in the continuum limit $G^c(n, \omega_b)$ are accurate up to 10^{-4}, and we obtain the results of table 1 ($\omega_b = 0.837\ \omega_d$). The Green's function are rapidly decreasing functions of $|n|$. Therefore, for a one-localized mode problem, we need only consider the central position of the localized mode and a few of its neighbours, in solving eqs. (5.6), (5.7) and (5.8). As we confined ourselves to a single-localized mode problem, let us assume that a localized mode exists at the origin $n = 0$ of the 1D lattice, its amplitude extending over its neighbouring atoms. A solution to the equation of physical interest is the s-like mode having the symmetry property: $\phi_n^i = \phi_{-n}^i$.

5.2. Numerical results

First we have to solve eqs. (5.6), (5.7) and (5.8) by iteration, starting with appropriate initial conditions. Using the result of the Fourier spectrum (fig. 6), we can determine the amplitude of each frequency in the resulting quasi-steady state found. The direct determination of the ϕ_n^i, knowing the frequency ω_b is theoretically possible, but we always find numerically the other (trivial) solution: $u_n = 0$, $\forall n$. To avoid this problem, we fix the dc term and determine the

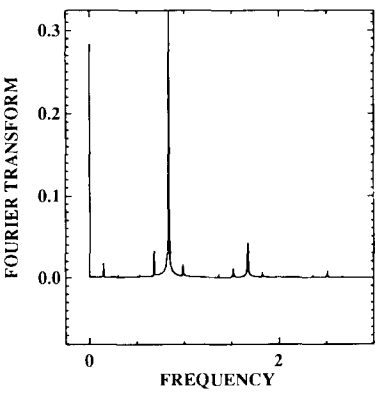

Fig. 6. Fourier transform of the breather oscillations. The frequency axis is in ω_d units. Noticed the dc component at $\omega = 0$, the frequency ω_b, its first and (weakly) second harmonic, and finally some of the $(n\omega_d + m\omega_b)$.

two sets of variables, ϕ_n^1 and ϕ_n^2 with eqs. (5.7) and (5.8). Only 15 iterations are necessary to determine the values with an accuracy of 10^{-4}, and because of the localization of the pulse and of the symmetry with respect to $n = 0$, it is only necessary to know a few values to obtain the result. In table 1, it is possible to compare the amplitude of each component of the Fourier spectrum, found in performing the Fourier transform of the simulation results, the Fourier series of the continuum solution and the result of the Green's function theory, for the oscillation's motion of the center of the breather and its first neighbour. This case corresponds to a breather frequency of $\omega_b = \omega_d$ (0.836 ± 0.006). From a value of $u_0^{max} = 0.88 \pm 0.04$, we get $u_0^{max} = 0.885$ as result of the method. We are now in position to make a numerical test of eq. (5.1) as approximate solution to eq. (2.3), by choosing as initial conditions $u_n(t = 0) = \phi_n^0 + \phi_n^1 + \phi_n^2$ and $\dot{u}_n(t = 0) = 0$. This is done by solving the last equation numerically with the same procedure as in section 4.

In fig. 7, we plot the maxima and the minima of the wave amplitude for the first three atoms ($n = 0, 1, 2$). Fig. 7a (respectively fig. 7b) corresponds to the evolution of the solution, determined with the continuum limit approximation (respectively Green's functions method). The comparison clearly shows that we are now extremely close to the exact discrete breather, whose existence is confirmed. The frequency of the breather is now $\omega_b = (0.837 \pm 0.003)\omega_d$. We can notice only a frequency difference, lower than 0.1% for the breather oscillation, which attests that the ansatz (5.1) approximates remarkably well the discrete breather profile. It is of course possible to take into account the third order term in the expansion, but the changes are less than 10^{-4}. To test the accuracy of the solution, we plot in fig. 8 the amplitude of the u_n at a distance of 50 units away from the center of the breather. We can see that the burst due to adaptation is clearly smaller in the second case; we note also that the amplitude is always 5×10^{-2} smaller than the maxima of oscillation of the

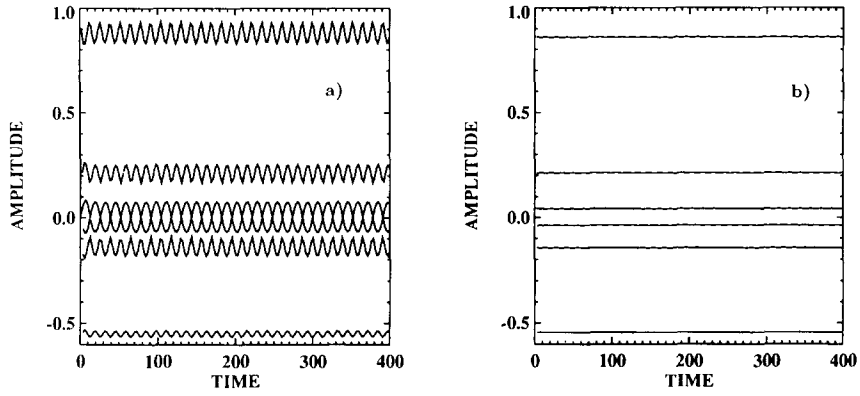

Fig. 7. Maxima and minima of amplitude oscillations for different particles; results of molecular dynamic simulations for the center of the breather and its two first neighbours. Simulation results with the continuum solution (a) and after using the Green's functions method (b).

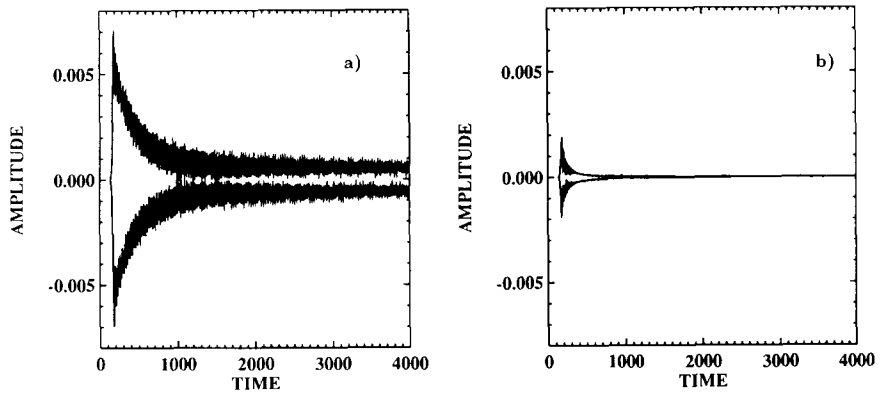

Fig. 8. u_n versus time for a particle at a distance of 50 units away from the center of the breather. Simulation results with the continuum solution (a) and after using the Green's functions method (b).

center. So, the modes obtained here are not exact eigenstates of the system, because we truncated the series, but we have obtained oscillating nonlinear localized modes with a very long lifetime.

6. Application to DNA

Let us now turn to the potential physical implications of our analysis, especially to model of DNA's breathing modes. The vibrational modes of stretching in DNA have been observed experimentally [16–18] and studied later theoretically [25,26], because they can induce melting by excessive stretching of the bonds. The striking connections between the properties of these openings and nonlinear phenomena studied before, has led to some related publications in the past ten years. These investigations have divided the biologist's community [27–29]; some of them recognized that this new and original approach was interesting and should be carried on.

As explained in a recent review [14], four significant variables (conformational, rotational, longitudinal and transverse changes) have been introduced in order to describe the main structural changes in DNA. Knowing the results of

new experiments, it has been recognized that the application of continuum methodology in the investigation of the nonlinear phenomena was maybe inadequate for the biological molecule of interest. The manifestations of the underlying discreteness cannot be predicted within the framework of the continuum approximation. In previous works [6,22], a model was introduced where each nucleotide of the double helix is presented by a point mass. The coupling, connecting those of the same strand were chosen to be harmonic, while the extremely stretched bonds between the two strands were modeled by a nonlinear potential. Using the motion about the center of mass of a nucleotide pair, we found the discrete nonlinear Hamiltonian (2.1). The original study used the Morse potential; the new one, having qualitatively the same profile for values lower than the local maximum of the 2–3 power potential [30,31] and keeping the asymmetry, allows us to define a stable state and an unstable state, whereas the Morse plateau prevents the breaking of the transversal bonds. The separation of the strands that is observed on heating the molecule shows that, when the thermal fluctuations are taken into account, the effective potential between the strands has a repulsive part when the strand separation exceeds some threshold. The 2–3 power potential is the first step in that direction before having a more suitable potential. Moreover, its curvature gives an oscillation's frequency which is a decreasing function of the amplitude. So the motion slows down, especially when the amplitude tends to the top of the potential, to stop when it reaches it. It is qualitatively in agreement with the soft-mode behavior of the breathing motion in DNA.

The estimate of model parameters adapted to the theory discussed in previous sections is not an easy step, but we have to check whether it is relevant to apply it to DNA. Consensually, the value relative to the nonlinear potential are fixed around the following values; the energy necessary to break the interstrand coupling is of the order of $E_0 = 0.1$ eV, whereas its limiting stretch is around $\alpha^{-1} = 0.5$ Å. Some previous studies used a more energetic interstrand coupling, taking into account only the H-bonds. But the nonlinear potential represents also the repulsive interactions which clearly diminish the potential barrier. The choice of the harmonic constant k is more controversial, and the values oscillate from 0.01 to 10 eV Å^{-2}. We have chosen $k = 0.3$ eV Å^{-2}, knowing the importance of discreteness effects in the macromolecule. This value gives a discreteness parameter of $\omega_d^2 = 6\alpha^2 E_0/k = 8$. The resulting behavior of the breathing motions will therefore be the one presented in the previous section. We obtain a very localized pulse, with a quasi-infinite lifetime and its stabilization is possible only because of the discreteness of the lattice as shown in the previous sections, in agreement with recent experimental results [4,5].

Finally, it is very important to know whether the dynamics of such modes is relevant to statistical mechanics of DNA, and the first thing we have to know is what is the ratio of the energy of one breather to $k_B T$. Taking always the same example we get $E \simeq 0.2$ eV and the breather energy $\simeq 6 k_B T$. Neglecting the asymmetry of the DNA chain, we can show [15,22] that u_n could represent the motion about the center of mass of a nucleotide pair. Keeping in mind that the motion in the phase of the two masses seems to be extremely small in comparison with the stretching, we can assume that the energy per site corresponds to $\simeq k_B T$. Therefore, knowing furthermore that the pulse is localized over a few particles, this result explains why the breather dynamics makes the dominant contributions in DNA, as indicated by the simulations of a similar model [8,32], and why this study is probably relevant for DNA.

7. Summary and conclusion

In this paper, we have concentrated on the ϕ^3 model, when the effects of the discreteness are

important. By studying the equations of motion of the system in the continuum limit we have obtained approximate expressions for the breather solutions. Numerical simulations have shown that these breathing modes are rather stable in the discrete cases, whereas an additional modulation phenomenon is present. From our results, it appears that the latter is due to the inexactitude of the solution. Owing to the importance of breathing motions in many physical applications, and particularly in DNA, we have developed a Green's function method to take account of the discreteness effects in detail. Searching long-lived oscillatory solutions, we find an accurate expression without the modulation. The agreement with the simulation, both qualitative and quantitative is a strong demonstration of the reliability of the formalism when the extent of the breather's length is of the order of the substrate lattice spacing. The main conclusion which emerges from our results is that the discreteness of the chain could be of great importance for a model, particularly when breather modes are involved. It confirms the hypothesis that it could be the fundamental reason of the stability of a localized solution.

Another point is that we have confined ourselves to the time evolution of harmonic lattices with a nonlinear on-site potential, associated with *static* localized modes. Propagative breather modes in this model are under consideration and will need the introduction of the collective variable approach [33,34]. Nontrivial combination effects of the additional Peierls–Nabarro potential and the breather oscillation will give rise to rich physics in this system.

Acknowledgements

We want to thank J.-M. Bilbault and R. Boesch for very helpful discussions. Part of this work has been supported by the EEC Science program under contract number SC1 0229-C (AM).

Appendix. Calculation of the Green's functions in the limit $N \to +\infty$

Replacing the sum over q by an integral over the first Brillouin zone, in the limit $N \to +\infty$, and denoting by $G^c(n, \omega_b)$ the expression of the Green's function obtained in the continuum limit, we get

$$G^c(n, \omega_b) = \frac{\omega_d^2}{2} \int_{-\pi}^{\pi} \frac{dq}{2\pi} \frac{\cos(nq)}{y - \cos(q)} = \frac{\omega_d^2}{2} \int_0^{\pi} \frac{dq}{\pi} \frac{\cos(nq)}{y - \cos(q)} . \tag{A.1}$$

A.1. Frequency in the gap

The integrand in eq. (7.1) is nonsingular and G may be easily evaluated by using the identity

$$\frac{1}{X} = \int_0^{+\infty} e^{-Xt} dt ;$$

we get therefore

$$G^c(n, \omega_b) = \frac{\omega_d^2}{2} \frac{1}{\pi} \int_0^{\pi} dq \cos(nq) \times \int_0^{+\infty} e^{-t[y - \cos(q)]} dt = \frac{\omega_d^2}{2} \int_0^{+\infty} dt\, e^{-yt} I_n(t) . \tag{A.2}$$

It is the Laplace transform of the Bessel function of imaginary argument I_n (see ref. [35]), i.e.

$$G^c(n, \omega_b) = \frac{\omega_d^2}{2} \frac{1}{\sqrt{y^2 - 1}} (y - \sqrt{y^2 - 1})^{|n|} . \tag{A.3}$$

The merit of the use of the method of lattice Green's function is easily seen from the explicit expression for $G^c(n, \omega_b)$.

A.2. Case of the first harmonic

The calculation of $G^c(n, 2\omega_b)$ is different because in that case $y < 1$. But for $(2\omega_b)^2 > \omega_b^2(\pi) = \omega_d^2 + 4$, we have $y < -1$; so $1/[y - \cos(q)]$ has no pole:

$$G^c(n, 2\omega_b) = \frac{\omega_d^2}{2} \int_0^\pi \frac{dq}{\pi} \frac{\cos(nq)}{y - \cos(q)}$$

$$= (-1)^n \frac{\omega_d^2}{2} \int_0^\pi \frac{d\theta}{\pi} \frac{\cos(n\theta)}{y + \cos(\theta)}$$

$$= -\frac{\omega_d^2}{2} \frac{1}{\sqrt{y^2 - 1}} \left(y + \sqrt{y^2 - 1}\right)^{|n|}, \tag{A.4}$$

References

[1] H. Segur and M.D. Kruskal, Phys. Rev. Lett. 58 (1987) 747.
[2] R.F. Dashen, B. Hasslacher and A. Neveu, Phys. Rev. D 11 (1975) 3424.
[3] E.M. Maslov, Phys. Lett. A 151 (1990) 47.
[4] M. Gueron, M. Kochoyan and J.L. Leroy, Nature 328 (1987) 89.
[5] J.L. Leroy, Regards sur la biochimie 5 (1990) 57.
[6] M. Peyrard, A. Bishop, Phys. Rev. Lett. A 62 (1989) 2755.
[7] C. Reiss, private communication (1991).
[8] M. Peyrard, T. Dauxois and H. Hoyet, Nanobiology Vol. 1, number 3.
[9] R. Boesch and M. Peyrard, Phys. Rev. B 43 (1991) 8491.
[10] D.K. Campbell and M. Peyrard, in: Chaos, Eds Campbell, Am. Inst. of Phys. (N.Y.) (1990) p. 305.
[11] M.J. Ablowitz, M.D. Kruskal and J.F. Ladik, SIAM J. Appl. Math. 36 (1979) 428.
[12] V.G. Makhankov, Phys. Rep. 35 (1978) 1.
[13] S. Takeno, K. Kisoda and A.J. Sievers, Prog. Theor. Phys. Suppl. 94 (1988) p. 242.
[14] G.Z. Zhou and C.T. Zhang, Phys. Sci. 43 (1991) 347.
[15] M. Techera, L.L. Daemen and E.W. Prohofsky, Phys. Rev. A 41 (1990) 4543.
[16] P.H. Bolton and T.L. James, J. Am. Chem. Soc. 102 (1980) 25.
[17] M.E. Hogan and O. Jardetzky, Biochemistry 19 (1980) 3460.
[18] D.P. Millar, R.J. Robbins and A.H. Zewail, Proc. Natl. Acad. Sci. (USA) 77 (1980) 5593.
[19] M. Remoissenet, Phys. Rev. B 33 (1986) 2386.
[20] C. Tatuam Kamga, J-B. Bilbault, M. Remoissenet, submitted to Phys. Rev.
[21] P.F. Byrd, in: Handbook of elliptic integrals for engineers and scientists, section 130.02, p. 30.
[22] T. Dauxois, Phys. Lett. A 159 (1991) 390.
[23] S. Takeno and K. Hori, J. Phys. Soc. Japan 60 (1991) 947.
[24] S. Takeno, J. Phys. Soc. Japan 59 (1990) 3861.
[25] E.W. Prohofsky et al., Phys. Lett. A 70 (1979) 492.
[26] B.F. Putnam, L.L. Van Zandt, E.W. Prohofsky and W.N. Mei, Biophysical J. 35 (1981) 271.
[27] J. Maddox, Nature 324 (1986) 11.
[28] M. Frank-Kamenetskii, Nature 328 (1987) 108.
[29] J. Maddox, Nature 339 (1989) 577.
[30] C.T. Zhang, J. Phys. Condens. Matter 2 (1990) 8259.
[31] W.G. Han and C.T. Zhang, J. Phys. Condens. Matter 3 (1991) 27.
[32] H. Hoyet and M. Peyrard, unpublished.
[33] R. Boesch, P. Stancioff and C.R. Willis, Phys. Rev. B 38 (1988) 6713.
[34] R. Boesch and C.R. Willis, Phys. Rev. B 42 (1990) 6371.
[35] M. Abramovitz and I.A. Stegun, in: Handbook of mathematical functions (Dover, NY) section 9.6.19.